Nuclear Engineering and Technology 53 (2021) 1634–1641

Contents lists available at ScienceDirect

Nuclear Engineering and Technology

journal homepage: www.elsevier.com/locate/net

Original Article

# Bentonite based ceramic materials from a perspective of gamma-ray shielding: Preparation, characterization and performance evaluation

Sinan Asal, Sema Akyil Erenturk*, Sevilay Haciyakupoglu

*Energy Institute, Istanbul Technical University, Maslak, 34469, Istanbul, Turkey*

ARTICLE INFO

*Article history:*
Received 10 July 2020
Received in revised form
4 November 2020
Accepted 4 November 2020
Available online 24 November 2020

*Keywords:*
Gamma-ray shielding
Bentonite
Ceramic
Attenuation coefficient
Half value thickness
Tenth value thickness

ABSTRACT

Exposure to gamma-rays is hazardous for humans and other living beings because of their high penetration through the materials. For this reason, shielding materials (usually lead, copper and stainless steel) are used to protect against gamma rays. This study's objective was to prepare ceramic materials for gamma radiation shielding by using different natural bentonite clays. Gamma-ray attenuation performances of the prepared shielding materials at different thicknesses were investigated and evaluated for different gamma-ray energies from different standard point gamma radiation sources ($^{251}$Am, $^{57}$Co, $^{137}$Cs, $^{60}$Co, and $^{88}$Y). The mass and linear attenuation coefficients of the prepared ceramics vary between 0.238 and 0.443 $cm^2\ g^{-1}$ and between 0.479 and 1.06 $cm^{-1}$, respectively, depending on their thicknesses. Results showed that these materials could be prioritized because of their evidential properties of gamma radiation protection in radiation applications.



## 1. Introduction

Gamma-ray is ionizing radiation with extremely short wavelengths and penetrates matter depending on the energy. Gamma radiation can also penetrate the human body and tissues quite easily and be hazardous to the human body, either external or internal. Biological effects in the human body from gamma radiation are deterministic effects and stochastic effects, creating DNA damage and cell death [1,2]. Radiation shielding materials have been developed to protect against potentially damaging effects of high-dose radiation exposure from gamma rays [3,4].

Initially, concretes and lead have widely used as radiation shielding material due to their effective shielding properties, cheap cost, high density, high mass attenuation and low maintenance. However, recently they don't meet the expectations for some nuclear technology applications due to their drawbacks such as poor mechanical properties, low chemical resistance, toxicity, and health hazards [2,5–7]. Based on the results of these studies, more investigations are needed about the shielding performances of different materials.

Many researchers have studied the usage possibility of natural rocks and minerals for the radiation shielding due to the low cost, and abundance [8–10]. Many new materials such as metal and alloys, composites, glasses and polymers have been produced as shielding materials in recent years [6,11–16]. Their performance against the ionizing radiation has been tested. Ceramics and ceramic composite materials are used in the shielding application against the ionizing radiation due to their features such as high thermal durability, mechanical strength, corrosion resistance, and low density [1,17–24]. Studies indicated that the shielding performance of the ceramics could be improved by testing new ceramic compounds.

This study aims to produce a ceramic shielding material that does not contain lead, has a low density and provides the necessary gamma-ray shielding performances by using the bentonite clay, which is abundant in our country and the world. In this frame, the ceramic matrix shielding materials at different material thicknesses were prepared and sintered at high temperatures. Their porosities, gamma-ray attenuation performances, half value thicknesses, and tenth value thicknesses for different gamma-ray energies were investigated and evaluated.

## 2. Material and method

### 2.1. Materials

Different types of bentonite clays taken from different provinces in Turkey were used to prepare the ceramic matrix materials to

* Corresponding author.
*E-mail address:* erenturk@itu.edu.tr (S.A. Erenturk).

https://doi.org/10.1016/j.net.2020.11.009

investigate their shielding properties against gamma radiation at different gamma-ray energies. Bentonite, a natural clay, deposits in the World, and Turkey is 6.2 million tons (metric) and 370,000 tons (metric) [25]. Bentonite includes various minerals like montmorillonite, quartz, feldspar, smectite, illite, kaolinite, calcite, chlorite, and pyrite. The percentage of these minerals may differ in each bentonite [26–28]. Bentonites used in the preparation of ceramic shielding are briefly named: RB for sodium bentonite from Resadiye-Tokat, AB for calcium bentonite from Karagedik-Ankara, SB calcium bentonite from Soma-Manisa, and CB for sodium and calcium bentonite from Çankırı.

### 2.2. Ceramic preparation

Natural bentonite clays were grinded - 74 μm size with a ball mill with a tungsten carbide bowl (Fusion Frequency FFBM-3A) and then passed through 40 μm sieve. The obtained mineral powders were left at 110 °C for 3 h in the oven (Heraeus D-6450) to remove the moisture. Each bentonite mineral was weighed as 7.5, 10, 15, and 20 g (Shimadzu Brand AUW220D) to investigate the material thickness's effect in the shielding characteristics. Then, the bentonite clays were homogenized in an agate mortar. Bentonite pellets were pressed at 40 MPa in the hydraulic press (Fusion Frequency) in 40 mm molds. After this procedure, each pellet was subject to sintering in high-temperature furnace (Nabertherm N7/h) carrying out with gradual temperature increase from room temperature to 600 °C at a 2 °C/min rate and held for two h. Then, the temperature was increased to 1100 °C at a 2 °C/min rate and held for 24 h. The sintered pellets were left to cool down overnight. After the sintering procedure, the thicknesses of prepared ceramics ranged between 3.2 and 8.08 mm related to their masses.

### 2.3. Gamma spectroscopic measurements

The gamma radiation shielding performance of sintered ceramic materials in various thicknesses was tested with the gamma transmission technique. The technique is based on the principle that detector and radioisotope are placed on two different sides of the material with the same axis. The detector measures the intensity of the radiation emitted from the gamma radiation sources after passing through the prepared shielding materials. At least two measurements were performed in the experiment with the radiation source and prepared ceramics. The gamma spectroscopy system consists of a copper-lined lead shielded (10 cm), n-type, vertical cryostat, coaxial pure germanium gamma detector (GAMMA-X HPGe) having 45.7% efficiency and integrated digital gamma spectrometer (DSPEC jr.2.0). Sample holder equipment and lead collimator shields given in Fig. 1 was used to keep the measuring distance and geometry constant. 3 mm of the collimator hole radius was used to create a narrow beam geometry and reduce the scattering effect. A point radiation source was placed at a distance of 18 cm from the bentonite ceramic. Spectrum analysis was performed using the Gamma Vision-32 software. The statistical confidence level and range were adjusted to 2σ and 8 K, respectively. Prepared samples and radiation sources were counted for time intervals from 3 min up to 30 min according to targeted counting statistics.

Gamma transmission properties of the ceramics were investigated by using $^{251}$Am, $^{57}$Co, $^{137}$Cs, $^{60}$Co, and $^{88}$Y standard gamma-ray point sources, which were obtained from Czech Metrology Institute-Inspectorate for Ionizing Radiation. The energy levels, intensities, and the minimum detectable activities of the used gamma-rays were given in Table 1. The minimum detectable activities (MDA) of the measurement system were calculated according to the Curie method [29,30]. Uncertainty sources consisting of calculations from the stages of sample preparation and gamma-ray measurements have a value between 1 and 10%. The minimum detectable activities (MDA) of the measurement system were calculated according to the Curie method [29,30]:

$$P = 1.645\frac{\sqrt{BG}}{t} \quad (1)$$

where P is the interested peak area, BG background radiation, t measurement time.

The gamma radiation sources activities vary between 6.666 and 17.58 kBq, and combined standard uncertainties vary between 0.4 and 1.0.

Uncertainty sources consisting of calculations from the stages of sample preparation and gamma-ray measurements for samples were considered. The uncertainty (u) of the activity ($A_x$) was calculated by the following equation:

$$u(A_x) = A_x \cdot \sqrt{\left(\frac{u(m_x)}{m_x}\right)^2 + \left(\frac{u(C_{x,w})}{C_{x,w}}\right)^2 + \left(\frac{u(C_{x,wo})}{C_{x,wo}}\right)^2} \quad (2)$$

where $u(C_{x,w})$ and $u(C_{x,wo})$ are the uncertainties of the net counts in the γ-ray peak of radionuclide in the ceramic sample with and without the radiation source and $u(m_x)$ the uncertainty of the mass from sample preparation step, respectively [29].

### 2.4. Calculating gamma attenuation

The activities obtained from the gamma source with and without the ceramic shielding material were used to calculate the linear attenuation coefficient (μ, usually measured in $cm^{-1}$ units) depending on the radiation energy according to Beer-Lambert's law [31–34]:

$$I = I_0 \exp(-\mu d) \quad (3)$$

where $I_0$ is the incoming photon intensity, I is the residual intensity after traversing radiation the material, and d is the absorber thickness (cm). These results were used to obtain the screening ratio (S; %) defined as the ratio of radiation intensity before and after interaction with the ceramic shielding material:

$$S = [(I_0 - I) / I_0] \times 100 \quad (4)$$

The density of the shielding material (ρ; g $cm^{-3}$) was determined by dividing the ceramic material's mass to the volume of the prepared ceramic material. The mass attenuation coefficient (μm; $cm^2$ $g^{-1}$) was obtained by dividing the linear attenuation coefficient to the material density:

$$\mu m = \mu / \rho \quad (5)$$

The half-value layer (HVL or $D_{1/2}$) and tenth value layer (TVL) definitions given in Equations (5) and (6) are important parameters for deciding of shielding properties of the ceramic materials:

$$HVL = \ln 2 / \mu \quad (6)$$

$$TVL = \ln 10 / \mu \quad (7)$$

These parameters can be expressed as the shielding material's thickness that can reduce the incoming radiation by half or ten. The TVL values are generally regarded as the lowest shielding thickness required for protection from the radiation source [28,30,31]. The percentage of heaviness (H) in equation (7) is another critical

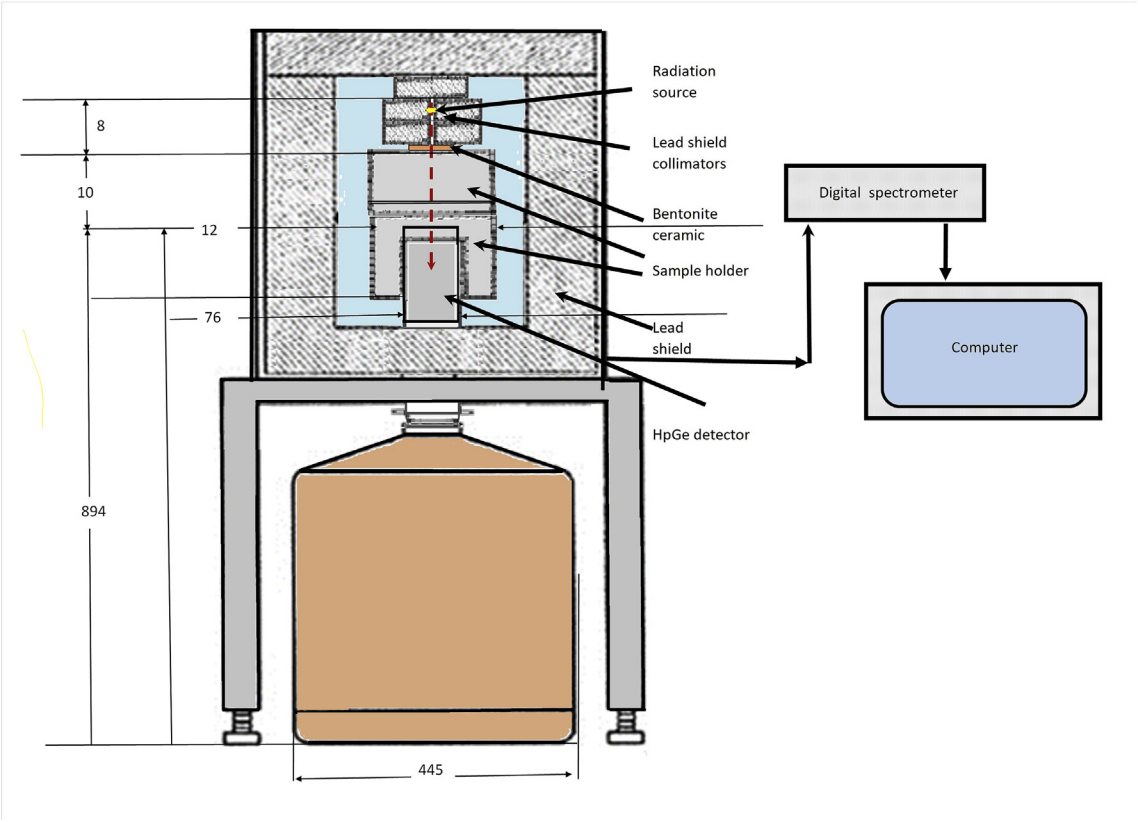


**Fig. 1.** Schematic presentation of experimental condition.

**Table 1**
Nuclear properties of used gamma-rays and system.

| Gamma source | Used Energy (keV) | Intensity (%) | MDA[a] (dpm)[b] |
|---|---|---|---|
| $^{241}$Am | 59.5 | 35.9 | 2 |
| $^{57}$Co | 122.1 | 85.60 | 1 |
| $^{137}$Cs | 661.7 | 85.10 | 2 |
| $^{60}$Co | 1173.2 | 99.859 | 2 |
| $^{60}$Co | 1332.5 | 99.9826 | 2 |
| $^{88}$Y | 1836.1 | 99.2 | 2 |

[a] Results are based on one hour count.
[b] dpm: disintegration per minute.

parameter that gives a measure of the lightness of the material when compared to a pure high atomic number component like lead [35–37].

$$H\ (\%) = (\text{Density of ceramic} \times 100) / (\text{Density of lead}) \quad (8)$$

### 2.5. Porosity determinations

Taking into account that the effective porosity of a liquid flows through the pores which are not connected in saturated pore media, the pore volume in the ceramic shielding materials are calculated by fluid saturation (Archimedes principle) from the mass of the liquid required to fill [39] by the following equation:

$$EP\ (\%) = [(w_c - w_a) / (w_c - w_b)] \times 100 \quad (9)$$

where $w_a$ is mass of dry sample in air, $w_b$ is suspended mass of water immersed sample in water and $w_c$ is the mass of water immersed sample in air.

### 2.6. Particle size determinations

Particle size can affect properties of the ceramic materials [36,38,40,41]. The small particle size provides more protection due to the possibility of radiation colliding with material atoms more [36,42]. The particle size distribution of the raw bentonite powder and ceramic materials were determined by a laser particle size analyser (Bettersiz BT-9300H) using Mie theory and data processing mode [43,44]. The detection range of the analyser is between 0.1 and 340 μm with 1% accuracy.

## 3. Results and discussion

Some properties of the ceramic shielding materials prepared from different types of bentonite were given in Table 2.

Table 2 shows that after the sintering process, the ceramic samples' mass loss varies between 11.5 and 20.4% according to the total mass and type of bentonite clays. Regarding the thermogravimetric analysis of bentonites, the changes caused by heating of the bentonite clays can be dehydration, dihydroxylation, and destruction of the clay mineral structure [45–47]. Densities of the ceramics materials varies between 1.58 and 2.15 g cm$^{-3}$ according to the mass and types of the bentonites. Comparison of the ceramic densities with the densities of other shielding materials (lead: 11.340 g cm$^{-3}$, tungsten: 19.11 g cm$^{-3}$ and bismuth 9.80 g cm$^{-3}$) reported by Abu Al Roos et al. (2019) indicates that low densities of the ceramics material will be advantageous for the gamma radiation shielding in many application fields [48].

**Table 2**
Properties of prepared bentonite ceramics.

| Bentonite ceramics | Total mass (g) | $T_{sint}$[a] (°C) | Mass loss (%) | ρ (g cm$^{-3}$) | Effective porosity (%) |
|---|---|---|---|---|---|
| RB-1 | 7.5 | 1100 | 12.53 | 1.58 | 0.54 |
| RB-2 | 10 | | 12.80 | 1.73 | 0.62 |
| RB-3 | 15 | | 12.73 | 2.04 | 0.75 |
| RB-4 | 20 | | 12.95 | 2.15 | 0.99 |
| AB-1 | 7.5 | 1100 | 20.13 | 1.77 | 0.75 |
| AB-2 | 10 | | 20.40 | 1.90 | 0.82 |
| AB-3 | 15 | | 20.13 | 1.94 | 0.95 |
| AB-4 | 20 | | 20.25 | 2.04 | 1.01 |
| SB-1 | 7.5 | 1100 | 14.13 | 1.77 | 0.71 |
| SB-2 | 10 | | 13.70 | 1.64 | 0.79 |
| SB-3 | 15 | | 13.53 | 1.88 | 0.96 |
| SB-4 | 20 | | 11.50 | 1.96 | 0.99 |

[a] $T_{sint}$: sintering temperature.

The heaviness of the ceramic materials varies between 13.90 and 18.99% of lead and this could increase the preference of ceramic materials as a shielding material in the future. Comparing the heaviness of the ceramic materials with some other shielding materials like steel, barite, concrete, modified polyethylene, and polyvinyl ether composites showed that the ceramic materials have lower heaviness than steel, barite and concrete and relative heaviness to modified polyethylene and polyvinyl ether composites [35,36]. The effective porosity values determined for each ceramic shielding materials were found to be less than 1%. These low porosity values contributed positively to compaction, densification, and shielding properties of prepared shielding materials [36,43].

Particle distribution of the raw material in ceramic production is one of the most important parameters in terms of ease of production and quality of the product. Therefore, D10, D50 and D90 values of the Gaussian curve showing the frequency distribution of the particles in the bentonites are given in Table 3. Here, the D90 values show the size that 90% of bentonite particles have. Similarly, the D50 is the size of which 50% of the bentonites is contained. The definition for D10 is then the size below which 10% of the bentonites is contained.

### 3.1. Effect of photon energy

The mass attenuation coefficient directly measures the effectiveness of a shielding material based upon the unit mass of material. Mass attenuation coefficients for the ceramic shielding materials in different thicknesses at the photon energies between 59.5 keV and 1836.1 keV were given in Fig. 2 a-d to indicate the effect of different bentonite clays on the photon attenuation. The values of the mass attenuation coefficients of the ceramic shielding materials vary between 0.238 and 0.443 cm$^2$ g$^{-1}$. On the other hand, the linear attenuation coefficients vary between 0.479 and 1.06 cm$^{-1}$.

It was seen that the performances of the ceramic shielding materials were substantially in a similar trend for all ceramic shielding materials. All mass attenuation coefficients showed a decrease with increasing photon energy. At low energies (lower than 661.7 keV), all ceramic materials showed high shielding performance. The mass attenuation coefficients for gamma energies from 661.7 to 1836.1 keV were nearly constant and very similar for all ceramic materials. Small differences in each ceramic material's attenuation properties can be due to minor differences in the basic compositions of the bentonite clays. Comparison of the mass attenuation coefficients of the ceramic shielding materials showed that the best performance for the ceramic materials at the selected gamma energies can be given in the following: SB ≥ RB ≥ AB ≥ CB.

Gamma-ray attenuation coefficients at 662, 1173, and 1332 keV energies were found higher than the reported in Ref. [42], and [49] for natural bentonite and bentonite with steel slag, respectively. Linear attenuation coefficients at 662, 1173, and 1332 keV gamma energies were reported as 0.067, 0.052, 0.048 cm$^{-1}$ by Hager et al., 2019 [42] and 0.150, 0.110 and 0.100 cm$^{-1}$ by Isfahan et al., 2018 [49]. These results indicate the positive impact of the applied sintering process to decrease porosity in the ceramic shielding materials. The photon energies of gamma and X-ray radiation for the common sources used by medicine vary from 5 keV to 511 keV [50,51]. It can be seen from the results that the prepared ceramic shielding materials can be a good choice for the gamma radiation shielding for medical applications. Additionally, the mass attenuation coefficients of the ceramic shielding materials were almost constant after the energy of the Cs-137 radioisotope (661.7 keV). This result can enable ceramics to be used in a wide range of energy in nuclear applications.

**Table 3**
Particle size distribution of used minerals.

| Mineral code | D10 (μm) | D50 (μm) | D90 (μm) |
|---|---|---|---|
| CB | 1.5 | 4.3 | 15.7 |
| SB | 1.9 | 8.3 | 36.3 |
| AB | 2.0 | 13.2 | 46.6 |
| RB | 2.3 | 13.6 | 61.1 |

### 3.2. Effect of thickness

The obtained screening ratio values evaluated the effect of thickness of the ceramic shielding materials on photon attenuation. Screening ratios of prepared ceramics varied between 17.156 and 35.243%. Curves for energy-mass attenuation coefficients have a turning point at the energy of 661.7 keV. A comparison of the screening rates of different ceramics with different thicknesses was given for only 661.7 keV in Fig. 3.

Curves in Fig. 3 show an increase (~40%) in screening ratio with the traversed thickness of all ceramic shielding materials. This trend is substantially similar for some other new offered shielding materials [35,52]. The screening ratio of the ceramic material produced in this study shows that the material's shielding properties have improved significantly, considering that it does not contain lead.

### 3.3. HVL and TVL values

The curves presented in Fig. 4 show an increase in the photon energy increasing up to the turning point (661.7 keV) and then

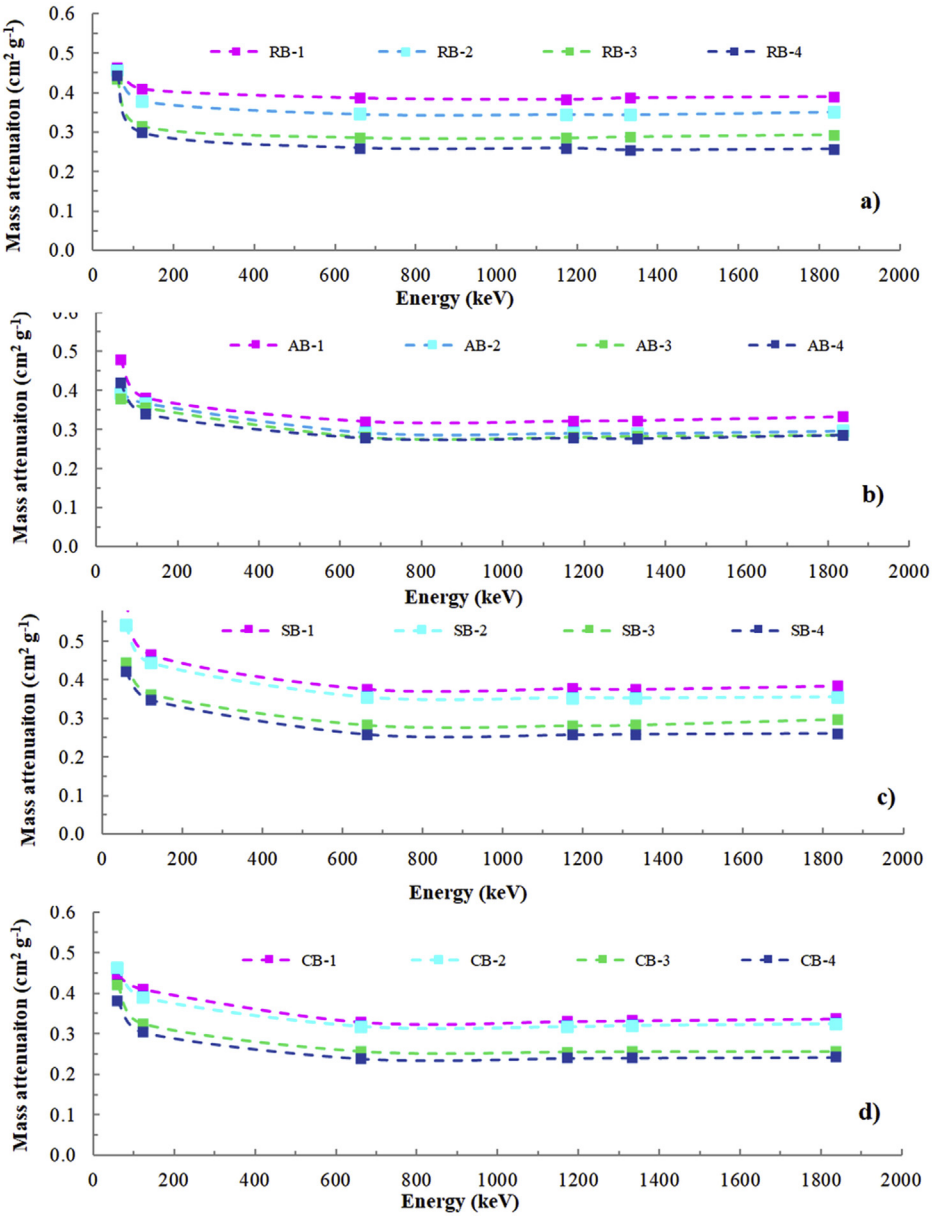


**Fig. 2.** Variation of the mass attenuation coefficients with the photon energy for a) RB, b) AB, c) SB, d) CB.

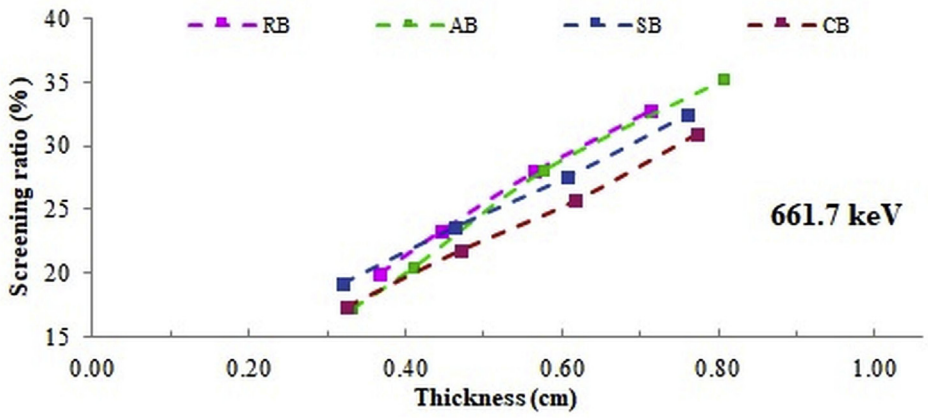


**Fig. 3.** Effect of material thickness for attenuating of photons at 661.7 keV energy.

progresses steadily in the researched range.

It can be considered that HLV of approximately 1.4 cm for the ceramic shielding materials could attenuate the photons with energies up to 1836.1 keV. The deviation between HVL and TVL of the ceramic shielding materials were shown for only 661.7 keV in Fig. 5 considering this energy is a turning point and could represent the trend for other energies.

The shielding performance of the ceramic materials was compared with other previously reported shielding materials to provide good evidence for the advantage of the investigated ceramic materials. HVL value was described between 2.53 and 9.17 cm for epoxy composites at 1173.2 and 1332.5 keV [38],

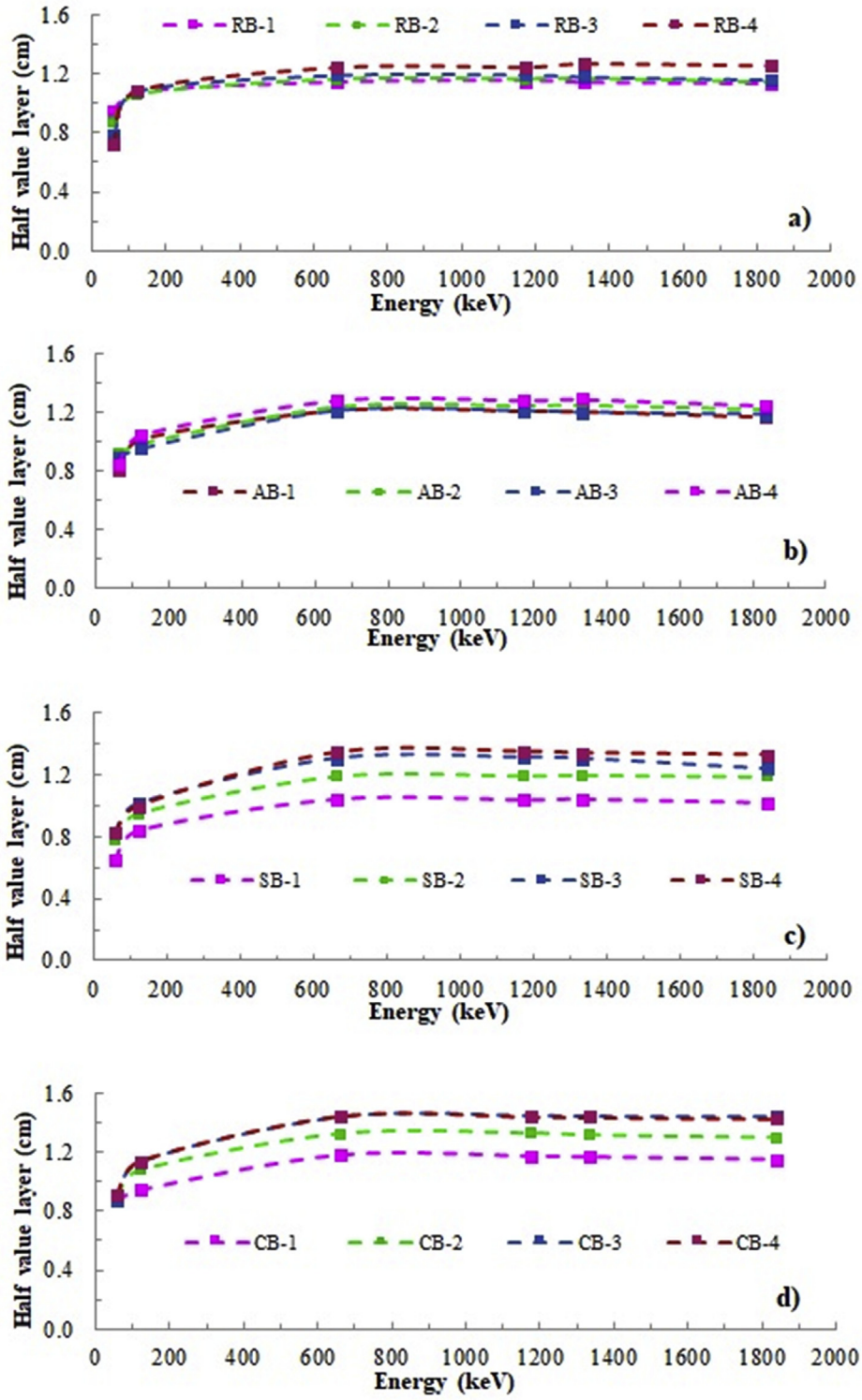


**Fig. 4.** The variation of HVL with photon energies for all bentonite types.

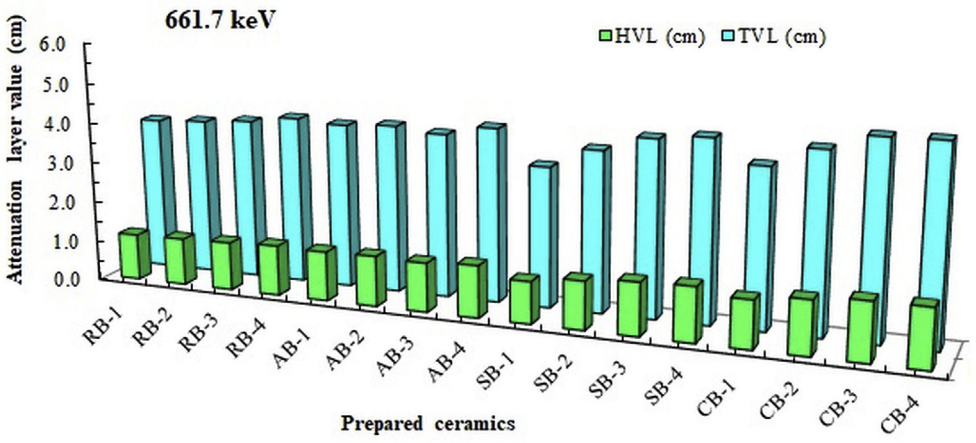


**Fig. 5.** HVL and TVL for used ceramic materials at selected photon energy.

5.669 cm for polycarbonate-bismuth nitrate composite at 511 keV [37] and 3.254 and 10.500 cm for lead doped polyethylene composites at 59.53 keV, and 1332.50 keV [36]. This value changes between 1.13 and 1.44 cm at 1173.2 and 1332.5 keV, 0.65, and 1.444 cm at 59.53 keV and 1332.50 keV for the ceramic shielding materials. As a result, the opportunity to use a thinner material compared to other shielding materials is an advantage for ceramic materials.

## 4. Conclusions

Gamma attenuation performance of the ceramic shielding materials prepared from natural bentonite clays obtained from different regions of Turkey was investigated and evaluated for radiation protection. The results obtained can be summarized under the following headings:

- Compared to the gamma attenuation performance of the raw bentonite at the same energies in the literature, the ceramic materials caused an increase in attenuation performance with decreasing the porosity in their structures by sintering the bentonites. The results of porosity tests indicate that the ceramics' effective porosity values were around $\leq$1%.
- Low densities and weights of the ceramic shielding materials could be one of the reasons to be preferred as a gamma shielding material over the conventional shielding materials.
- The mass or linear attenuation coefficients of the ceramic materials are relatively higher than those of conventional shielding materials. They showed a slight decrease with increasing gamma-ray energy. This feature allows the ceramic materials to be used in a wide energy interval.
- An increase in the thickness of the ceramic materials showed an increase in screening ratios that could make it possible to prepare shields with required properties.
- HVL and TVL values show that ceramic materials can shield photons of a wide range of energies within a short distance.

Due to the abundance of bentonites in the world and toxicity of lead, one of the most used conventional shielding materials, bentonite-based ceramic materials could be chosen in radiation protection applications to protect people from harmful and dangerous effects of gamma radiation. Bentonite ceramics can be used a shielding material in medical and industrial applications.

## Declaration of competing interest

The authors declare that they have no known competing financial interests or personal relationships that could have appeared to influence the work reported in this paper.

## Acknowledgements

This work is part of the project supported by the Istanbul Technical University Research Foundation (Project No: 39416). We gratefully acknowledge Czech Metrology Institute-Inspectorate for Ionizing Radiation for providing the standard gamma-ray point sources.

## References

[1] F. Akman, Z.Y. Khattari, M.R. Kaçal, M.I. Sayyed, F. Afaneh, The radiation shielding features for some silicide, boride and oxide types ceramics, Radiat. Phys. Chem. 160 (2019) 9–14.
[2] F. Akman, M.R. Kaçal, M.I. Sayyed, H.A. Karata, Study of gamma radiation attenuation properties of some selected ternary alloys, J. Alloys Compd. 782 (2019) 315–322.
[3] G. Hu, H. Hu, Q. Yang, B. Yu, W. Sun, Study on the design and experimental verification of multilayer radiation shield against mixed neutrons and γ-rays, Nucl. Eng. Technol. 52 (1) (2020) 178–184.
[4] C.G. Hernandez-Murillo, J.R.M. Contreras, L.A. Escalera-Velasco, H.A. de Leon-Martínez, H.R. Vega-Carrillo, X-ray and gamma ray shielding behavior of concrete blocks, Nucl. Eng. Technol. 52 (8) (2020) 1792–1797.
[5] K.J. Singh, N. Singh, R.S. Kaundal, K. Singh, Gamma-ray shielding and structural properties of PbO–$SiO_2$ glasses, Ann. Nucl. Energy 64 (2014) 301–310.
[6] B. Ahmed, G.B. Shah, A.H. Malik, R.M. Aurangzeb, Gamma-ray shielding characteristics of flexible silicone tungsten composites, Appl. Radiat. Isot. 155 (2020) 108901.
[7] F. Cattant, D. Crusset, D. Féron, Corrosion issues in nuclear industry today, Mater. Today 11 (10) (2008) 32–37.
[8] A. Mansour, M.I. Sayyed, K.A. Mahmoud, E. Şakar, E.G. Kovaleva, Modified halloysite minerals for radiation shielding purposes, J. Radiat. Res. Appl. Sc. 13 (1) (2020) 94–101.
[9] M.I. Sayyed, A. Kumar, H.O. Tekin, R. Kaur, M. Singh, O. Agar, M.U. Khandaker, Evaluation of gamma-ray and neutron shielding features of heavy metals doped $Bi_2O_3$-BaO-$Na_2O$-MgO-$B_2O_3$ glass systems, Prog. Nucl. Energy 118 (2020) 103118, https://doi.org/10.1016/j.pnucene.2019.103118.
[10] S.S. Obaid, M.I. Sayyed, D.K. Gaikwad, P.P. Pawar, Attenuation coefficients and exposure buildup factor of some rocks for gamma ray shielding applications, Radiat. Phys. Chem. 148 (2018) 86–94.
[11] T. Kaur, J. Sharma, T. Singh, Review on scope of metallic alloys in gamma rays shield designing, Prog. Nucl. Energy 113 (2019) 95–113.
[12] C.V. More, R.R. Bhosale, P.P. Pawar, Detection of new polymer materials as gamma-ray-shielding materials, Radiation Effects and Defects in Solids, Incorporating Plasma Science and Plasma Technology 172 (5–6) (2017) 469–484.
[13] S.A.M. Issa, A.M. Ali, H.O. Tekin, Y.B. Saddeek, A. Al-Hajry, H. Algarni, G. Susoy, Enhancement of nuclear radiation shielding and mechanical properties of $YBiBO_3$ glasses using $La_2O_3$, Nucl. Eng. Technol. 52 (2020) 1297–1303.

[14] M.I. Sayyed, H.O. Tekin, O. Kılıcoglu, O. Agar, M.H.M. Zaid, Shielding features of concrete types containing sepiolite mineral: comprehensive study on experimental, XCOM and MCNPX results, Results in Physics 11 (2018) 40–45.
[15] A. Levet, E. Kavaz, Y. Ozdemir, An experimental study on the investigation of nuclear radiation shielding characteristics in iron-boron alloys, J. Alloys Compd. 819 (2020) 152946, https://doi.org/10.1016/j.jallcom.2019.152946.
[16] V.P. Singh, N.M. Badiger, Gamma ray and neutron shielding properties of some alloy materials, Ann. Nucl. Energy 64 (2014) 301–310.
[17] M.R. Kacal, F. Akman, M.I. Sayyed, Investigation of radiation shielding properties for some ceramics, Radiochim. Acta 107 (2) (2018) 179–191.
[18] M. Gorbotenko, Y. Yuferev, Ceramicrete as a Means for Radioactive Waste Containment and Nuclear Shielding, Reports by All-Russian Research Institute of Experimental Physics Federation, to Argonne National Laboratory, Sarov, Russian, 2002.
[19] A.S. Wagh, S.Y. Sayenko, A. Dovbnya, V. Shkuropatenko, R. Tarasov, A. Rybka, A. Zakharchenko, Durability and shielding performance of borated ceramicrete coatings in beta and gamma radiation fields, J. Nucl. Mater. 462 (2015) 165–172.
[20] S. Mahmoudi, A. Bennour, A. Meguebli, E. Srasra, F. Zargouni, Characterization and traditional ceramic application of clays from the Douiret region in South Tunisia, Appl. Clay Sci. 127–128 (2016) 78–87.
[21] M.E. Mahmoud, A.M. El-Khatib, A.M. Halbas, R.M. El-Sharkawy, Investigation of physical, mechanical and gamma-ray shielding properties using ceramic tiles incorporated with powdered lead oxide, Ceram. Int. 46 (2020) 15686–15694.
[22] J. Klimke, M. Trunec, A. Krell, Transparent tetragonal Yttria-stabilized zirconia ceramics: influence of scattering caused by birefringence, J. Am. Ceram. Soc. 94 (6) (2011) 1850–1858.
[23] R.R. Enrique, A.R.G. José, E.V. Sergio, C.S. Brianda, E.G. Ivanovich, M.S. Roberto, Effect of particle size and titanium content on the fracture toughness of particle-ceramic composites, Mater. Today, Proceedings 3 (2016) 249–257.
[24] E. Kavaz, F.I. El_Agawany, H.O. Tekin, U. Perisanoglu, Y.S. Rammah, Nuclear radiation shielding using barium borosilicate glass ceramics, J. Phys. Chem. Solid. 142 (2020) 109437.
[25] British Geological Survey, World Mineral Production, 2008-12, British Geological Survey, 2012. Keyworth, Nottingham.
[26] G. Bulut, M. Chimeddorj, F. Esenli, M.S. Çelik, Production of desiccants from Turkish bentonites, Appl. Clay Sci. 46 (2009) 141–147.
[27] E. Cokca, Z. Yilmaz, Use of rubber and bentonite added fly ash as a liner material, Waste Manag. 24 (2004) 153–164.
[28] H. Akgün, A.G. Türkmenoglu, İ. Met, G.P. Yal, M.K. Koçkar, The use of Ankara Clay as a compacted clay liner for landfill sites, Clay Miner. 52 (2017) 391–412.
[29] N. Tsoulfanidis, S. Landsberger, Measurement and Detection of Radiation, third ed., CRC Press, Boca Raton, 2010.
[30] ORTEC, GMX Series Coaxial HPGe Detector Product Configuration Guide, 2003.
[31] L. Chang, Y. Zhang, Y. Liu, J. Fang, W. Luan, X. Yang, W. Zhang, Preparation and characterization of tungsten/epoxy composites for γ-rays radiation shielding, Nucl. Instrum. Methods B. 356–357 (2015) 88–93.
[32] J.E. Martin, Physics for Radiation Protection, Markono Print Media Pte Ltd, Singapore, 2013.
[33] R.B. Firestone, in: A. Vértes, S. Nagy, Z. Klencsár, R.G. Lovas, F. Rösch (Eds.), Handbook of Nuclear Chemistry, Springer, Berlin, 2011.
[34] J.E. Turner, Atoms, Radiation, and Radiation Protection, Wiley, New York, 2007.
[35] M.M. El-Toony, G. Eid, H.M. Algarnic, T.F. Alhawimald, E.E. Abel-Hady, Synthesis and characterisation of smart poly vinyl ester/$Pb_2O_3$ nanocomposite for gamma radiation shielding, Radiat. Phys. Chem. 168 (2020) 108536, https://doi.org/10.1016/j.radphyschem.2019.108536.
[36] M.E. Mahmoud, A.M. El-Khatib, M.S. Badawi, A.R. Rashad, R.M. El-Sharkawy, A.A. Thabet, Recycled high-density polyethylene plastics added with lead oxide nanoparticles as sustainable radiation shielding materials, Radiat. Phys. Chem. 145 (2018) 160–173.
[37] R. Mirji, B. Lobo, Study of polycarbonate–bismuth nitrate composite for shielding against gamma radiation, J. Radioanal. Nucl. Chem. 324 (2020) 7–19.
[38] L. Chang, Y. Zhang, Y. Liu, J. Fang, W. Luan, X. Yang, W. Zhang, Preparation and characterization of tungsten/epoxy composites for γ-rays radiation shielding, Nucl. Instrum. Methods B. 356–357 (2015) 88–93.
[39] O. Yazici, Investigation of Sol-Gel Derived Spinel Added Alumina Low Cement Castable Refractories, 2008, p. 52. MSc Thesis (in Turkish).
[40] W. Cheewasukhanont, P. Limkitjaroenporn, S. Kothan, C. Kedkaew, J. Kaewkhao, The effect of particle size on radiation shielding properties for bismuth borosilicate glass, Radiat. Phys. Chem. 172 (2020) 108791, https://doi.org/10.1016/j.radphyschem.2020.108791.
[41] A.E. Abdo, M.A. El-Sarraf, F.A. Gaber, Utilization of ilmenite/epoxy composite for neutrons and gamma rays attenuation, Ann. Nucl. Energy 30 (2003) 175–187.
[42] I. Hager, Y.S. Rammah, H.A. Othman, E.M. Ibrahim, S.F. Hassan, Nano-structured natural bentonite clay coated by polyvinyl alcohol polymer for gamma rays attenuation, J. Theor. Appl. Phys. 13 (2019) 141–153.
[43] R.R. Enrique, A.R.G. José, E.V. Sergio, C.S. Brianda, E.G. Ivanovich, M.S. Roberto, Effect of particle size and titanium content on the fracture toughness of particle-ceramic composites, Mater. Today, Proceedings 3 (2016) 249–257.
[44] J. Klimke, M. Trunec, A. Krell, Transparent tetragonal Yttria-stabilized zirconia ceramics: influence of scattering caused by birefringence, J. Am. Ceram. Soc. 94 (6) (2011) 1850–1858.
[45] S. Stojiljković, M. Stamenković, D. Kostić, M. Miljković, B. Arsić, I. Savić, I. Savić, Investigations of the changes in the bentonite structure caused by the different treatments, Sci. Sinter. 47 (2015) 51–59.
[46] H.H. Murray, Bentonite applications, in: Developments in Clay Science, vol. 2, Elsevier, New York, 2006, pp. 111–130.
[47] G. Bulut, M. Chimeddorj, F. Esenli, M.S. Çelik, Production of desiccants from Turkish bentonites, Appl. Clay Sci. 46 (2009) 141–147.
[48] N.J. AbuAlRoos, N.A.B. Amin, R. Zainon, Conventional and new lead-free radiation shielding materials for radiation protection in nuclear medicine: a review, Radiat. Phys. Chem. 165 (2019) 108439.
[49] H.S. Isfahani, S.M. Abtahi, M.A. Roshanzamir, A. Shirani, S.M. Hejazi, Investigation on gamma-ray shielding and permeability of clay-steel slag mixture, Bull. Eng. Geol. Environ. 78 (2019) 4589–4598.
[50] Radioisotopes in Medicine, https://www.world-nuclear.org/information-library/non-power-nuclear-applications/radioisotopes-research/radioisotopes-in-medicine.aspx (accessed 12 Mar 2020).
[51] S. Mirzadeh, L.F. Mausner, M.A. Garland, A. Veŕtes, S. Nagy, Z. Klencsaŕ, R.G. Lovas, F. Rösch (Eds.), Handbook of Nuclear Chemistry, Springer, Berlin, 2011.
[52] M.H. Kharita, M. Takeyeddin, M. Alnassar, S. Yousef, Development of special radiation shielding concretes using natural local materials and evaluation of their shielding characteristics, Prog. Nucl. Energy 50 (2008) 33–36.